

Discussions on driven cavity flow and steady solutions at high Reynolds numbers

Ercan Erturk

*Energy Systems Engineering Department, Gebze Institute of Technology,
Gebze, Kocaeli 41400, Turkey*

Keywords Driven Cavity Flow, Steady 2-D Incompressible N-S Equations, Fine Grid Solutions, High Reynolds Numbers

Abstract The numerical solutions of 2-D steady incompressible flow in a driven cavity are presented. The Navier-Stokes equations in streamfunction and vorticity variables are solved simply with Successive Over Relaxation (SOR) method. Using a very fine grid mesh with 1025×1025 points, the steady driven cavity flow is solved for $Re \leq 20,000$. For accuracy, the iterations are carried out on the streamfunction and vorticity variables until the steady streamfunction and vorticity equations are satisfied with a residual that were less than 10^{-10} . Interesting features of the flow are presented in detail. The driven cavity flow at high Reynolds numbers is discussed in detail in terms of physical and mathematical and also numerical aspects.

1. INTRODUCTION

The lid driven cavity flow is most probably one of the most studied fluid problems in computational fluid dynamics field. The simplicity of the geometry of the cavity flow makes the problem easy to code and apply boundary conditions and etc. Even though the problem looks simple in many ways, the flow in a cavity retains all the flow physics with counter rotating vortices appear at the corners of the cavity.

Driven cavity flow serve as a benchmark problem for numerical methods in terms of accuracy, numerical efficiency and etc. In the literature it is possible to find numerous studies on the driven cavity flow. The numerical studies on the subject of driven cavity flow can be basically grouped into three categories;

1. In the first category of studies, the *steady* solution of the driven cavity is sought. In these type of studies the numerical solution of steady incompressible Navier-Stokes equations are presented at various Reynolds numbers. Erturk et. al. [12], Erturk and Gokcol [13], Barragy & Carey [4], Schreiber & Keller [37], Benjamin & Denny [6], Liao & Zhu [28], Ghia et. al. [21] are examples of steady driven cavity flow studies at high Reynolds numbers.

Email: ercanerturk@gyte.edu.tr
URL: <http://www.cavityflow.com>

Download figures, tables, data files, fortran codes and etc. All the numerical solutions presented in this study are available to public in this web site.

2. In the second category of studies, the bifurcation of the flow in a driven cavity from a steady regime to an unsteady regime is studied. In these studies a hydrodynamic stability analysis is done and the Reynolds numbers at which a Hopf bifurcation occurs in the flow are presented. Fortin et. al. [19], Gervais et. al. [20], Sahin & Owens [35] and Abouhamza & Pierre [1] are examples of hydrodynamic stability studies on driven cavity flow.
3. In the third category of studies, the transition from steady to unsteady flow is studied through a Direct Numerical Simulation (DNS) and the transition Reynolds number is presented. Auteri, Parolini & Quartapelle [2], Peng, Shiao & Hwang [30], Tiesinga, Wubs & Veldman [42], Poliashenko & Aidun [32], Cazemier, Verstappen & Veldman [8], Goyon [22], Wan, Zhou & Wei [44] and Liffman [29] are examples of DNS studies on driven cavity flow.

Even though the driven cavity flow is studied at this extent in the literature, there are some points that are still not agreed upon. As it will be discussed briefly in the following sections, the studies in the second category with hydrodynamic stability analysis and the studies in the third category with Direct Numerical Simulation claim that the driven cavity flow undergoes a Hopf bifurcation after a Reynolds number, and most importantly they claim that, beyond this Reynolds number the flow in a driven cavity is unsteady therefore a steady solution does not exist hence a steady solution at high Reynolds numbers is not computable. However there are also many studies in the first category that present steady solutions at Reynolds numbers higher than the transition Reynolds numbers predicted by the second and third category of studies. For the driven cavity flow problem there is a controversy at high Reynolds numbers such that some studies predict that the flow is time dependent and a steady solution does not exist, while some other studies presents steady solutions.

Based on the studies we found in the literature, we conclude that there are some confusions on the subject of driven cavity flow. We believe that for this flow problem some important points have to be discussed and analyzed and agreed upon, such as;

- The physical nature of the flow in a driven cavity especially at high Reynolds numbers.
- The transition Reynolds number from a steady flow to unsteady flow.
- Whether or not there exists a steady solution for driven cavity at high Reynolds numbers.
- The significance of a study that analyze the Hopf bifurcation in a driven cavity through a hydrodynamic stability analysis.
- The significance of a study that analyze the transition Reynolds number in a driven cavity through a Direct Numerical Simulation.
- The significance of a study that presents steady solutions of driven cavity at high Reynolds numbers.

The main purpose of this study is then to discuss the incompressible flow in a 2-D driven cavity in terms of physical, mathematical and numerical aspects, together with a

very brief literature survey on experimental and numerical studies. We will also present very fine grid steady solutions of the driven cavity flow at very high Reynolds numbers. Based on the results obtained, we will analyze the nature of the flow in a driven cavity in an attempt to address the controversy on this flow problem.

2. PROBLEM FORMULATION AND NUMERICAL ALGORITHM

As the starting point of problem formulation, we assume that the incompressible flow in a driven cavity is *two-dimensional*. A second point is that, we are seeking a *steady* solution. After these two starting points, the problem at hand is governed by the 2-D steady incompressible Navier-Stokes equations. We use the governing equations in streamfunction (ψ) and vorticity (ω) formulation such that

$$\frac{\partial^2 \psi}{\partial x^2} + \frac{\partial^2 \psi}{\partial y^2} = -\omega \quad (1)$$

$$\frac{1}{\text{Re}} \left(\frac{\partial^2 \omega}{\partial x^2} + \frac{\partial^2 \omega}{\partial y^2} \right) = \frac{\partial \psi}{\partial y} \frac{\partial \omega}{\partial x} - \frac{\partial \psi}{\partial x} \frac{\partial \omega}{\partial y} \quad (2)$$

These equations are non-dimensional, where Re is the Reynolds number, and x and y are the Cartesian coordinates.

The above equations are solved with a very well known numerical method, the Successive Over Relaxation (SOR) method. SOR method is most probably the simplest and the most easy to apply numerical method. The reason why we have chosen SOR method is that we would like to demonstrate even the simplest explicit method is capable of producing a result at very high Reynolds numbers. For the cavity flow problem, the solver is less than 30 lines of Fortran code. The solution methodology is quite simple. First an initial guess is assigned to $\psi_{i,j}$ and $\omega_{i,j}$ where i and j are the grid index in x- and y-direction respectively. As an initial guess either a homogeneous solution can be used or alternatively for a given Reynolds number, a previously obtained smaller Reynolds number solution can be used. The grids are numbered from 0 to N where N is the number of grids points. Same number of grid points is used in x- and y-directions. Then in a nested loop of

DO $i=1,N-1$

DO $j=1,N-1$

the streamfunction variable is advanced using the following equation

$$\psi_{i,j}^{n+1} = \beta \left(0.25(\psi_{i-1,j}^{n+1} + \psi_{i,j-1}^{n+1} + \psi_{i+1,j}^n + \psi_{i,j+1}^n + h^2 \omega_{i,j}) \right) + (1 - \beta) \psi_{i,j}^n \quad (3)$$

where h is the grid spacing ($\Delta x = \Delta y = h$) and β is the relaxation parameter. The streamfunction value at the wall is zero.

The vorticity values at the wall is calculated using Jensen's formula (see Fletcher [16])

$$\omega_0 = \frac{-4\psi_1 + 0.5\psi_2}{h^2} - \frac{3V}{h} \quad (4)$$

where subscript 0 refers to the points on the wall and 1 refers to the points adjacent to the wall and 2 refers to the second line of points adjacent to the wall and also V refers to the velocity of the wall with being equal to 1 on the moving top wall and 0 on the other three stationary walls. Then similarly, in a nested loop

DO $i=1,N-1$
 DO $j=1,N-1$

the vorticity variable is advanced using the following equations

$$\begin{aligned} \omega_{i,j}^{n+1} = \beta & \left(0.25 \left(\omega_{i-1,j}^{n+1} + \omega_{i,j-1}^{n+1} + \omega_{i+1,j}^n + \omega_{i,j+1}^n - 0.25 \operatorname{Re} (\psi_{i,j+1} - \psi_{i,j-1}) (\omega_{i+1,j}^n - \omega_{i-1,j}^{n+1}) \right. \right. \\ & \left. \left. + 0.25 \operatorname{Re} (\psi_{i+1,j} - \psi_{i-1,j}) (\omega_{i,j+1}^n - \omega_{i,j-1}^{n+1}) \right) \right) + (1 - \beta) \omega_{i,j}^n \end{aligned} \quad (5)$$

During the iterations, as a measure of the convergence to the steady state, we monitored three residual parameters. The first residual parameter, RES1 , is defined as the maximum absolute residual of the finite difference equations of steady streamfunction and vorticity equations (1 and 2). These are respectively given as

$$\begin{aligned} \text{RES1}_\psi &= \max \left(\left| \frac{\psi_{i-1,j}^{n+1} - 2\psi_{i,j}^{n+1} + \psi_{i+1,j}^{n+1}}{h^2} + \frac{\psi_{i,j-1}^{n+1} - 2\psi_{i,j}^{n+1} + \psi_{i,j+1}^{n+1}}{h^2} + \omega_{i,j}^{n+1} \right| \right) \\ \text{RES1}_\omega &= \max \left(\left| \frac{1}{\operatorname{Re}} \frac{\omega_{i-1,j}^{n+1} - 2\omega_{i,j}^{n+1} + \omega_{i+1,j}^{n+1}}{h^2} + \frac{1}{\operatorname{Re}} \frac{\omega_{i,j-1}^{n+1} - 2\omega_{i,j}^{n+1} + \omega_{i,j+1}^{n+1}}{h^2} \right. \right. \\ & \left. \left. - \frac{\psi_{i,j+1}^{n+1} - \psi_{i,j-1}^{n+1}}{2h} \frac{\omega_{i+1,j}^{n+1} - \omega_{i-1,j}^{n+1}}{2h} + \frac{\psi_{i+1,j}^{n+1} - \psi_{i-1,j}^{n+1}}{2h} \frac{\omega_{i,j+1}^{n+1} - \omega_{i,j-1}^{n+1}}{2h} \right| \right) \end{aligned} \quad (6)$$

We think that among the three residual parameters we have used, RES1 is the most important residual parameters. The magnitude of RES1 is an indication of the degree to which the solution has converged to steady state. In the limit RES1 would be zero.

The second residual parameter, RES2 , is defined as the maximum absolute difference between two iteration steps in the streamfunction and vorticity variables. These are respectively given as

$$\begin{aligned} \text{RES2}_\psi &= \max \left(\left| \psi_{i,j}^{n+1} - \psi_{i,j}^n \right| \right) \\ \text{RES2}_\omega &= \max \left(\left| \omega_{i,j}^{n+1} - \omega_{i,j}^n \right| \right) \end{aligned} \quad (7)$$

RES2 gives an indication of the significant digit on which the code is iterating.

The third residual parameter, RES3 , is similar to RES2 , except that it is normalized by the representative value at the previous time step. RES3 is defined as

$$\begin{aligned} \text{RES3}_\psi &= \max \left(\left| \frac{\psi_{i,j}^{n+1} - \psi_{i,j}^n}{\psi_{i,j}^n} \right| \right) \\ \text{RES3}_\omega &= \max \left(\left| \frac{\omega_{i,j}^{n+1} - \omega_{i,j}^n}{\omega_{i,j}^n} \right| \right) \end{aligned} \quad (8)$$

RES3 gives an indication of the maximum percent change in the streamfunction and vorticity variable in each iteration step. Note that, when a homogeneous initial guess is used, then in the first iteration, calculation of RES3 is skipped since $\psi_{i,j}$ and $\omega_{i,j}$ is homogeneous.

In our calculations, for all Reynolds numbers we considered that convergence was achieved when both $\text{RES1}_\psi \leq 10^{-10}$ and $\text{RES1}_\omega \leq 10^{-10}$ was achieved. Such a low value was chosen to ensure the accuracy of the solution. At these convergence levels the second residual parameters were in the order of $\text{RES2}_\psi \leq 10^{-17}$ and $\text{RES2}_\omega \leq 10^{-15}$, that means the streamfunction and vorticity variables are accurate to 16th and 14th digit accuracy respectively at a grid point and even more accurate at the rest of the grids. Also at these convergence levels the third residual parameters were in the order of $\text{RES3}_\psi \leq 10^{-14}$ and $\text{RES3}_\omega \leq 10^{-13}$, that means the streamfunction and vorticity variables are changing with 10⁻¹²% and 10⁻¹¹% of their values respectively in an iteration step at a grid point and even with less percentage at the rest of the grids. Obviously these convergence levels are far more less than satisfactory and one would think that such low values are not necessary. One of the reasons why we let the iterations converge to these levels was to demonstrate that for the driven cavity flow even a basic SOR algorithm is capable of achieving such low residual values at high Reynolds numbers when a fine grid mesh is used. During the iterations the three residual parameters steadily decrease without any oscillations.

The number of grid points used in this study is 1025×1025 .

3. RESULTS

The boundary conditions and a schematics of the vortices generated in a driven cavity flow are shown in Figure 1. In this figure, the abbreviations BR, BL and TL refer to bottom right, bottom left and top left corners of the cavity, respectively. The number following these abbreviations refer to the vortices that appear in the flow, which are numbered according to size. Erturk et. al. [12] have presented an efficient numerical method and with using their numerical method they have presented steady solutions of the cavity flow up to Reynolds number of 21,000 using fine grid mesh. They have clearly stated that in order to obtain a steady solutions at high Reynolds numbers ($\text{Re} > 10,000$), a grid mesh larger than 257×257 have to be used. We have decided to test the validity of their statement using the SOR algorithm. The SOR algorithm is an explicit algorithm and it is most probably the easiest algorithm in terms of coding. First we start with a grid mesh of 257×257 . With this many grid points we have obtained steady solutions up to Reynolds number of 7,500 however no matter how small we choose the relaxation parameters we could not obtain a steady solution above this Reynolds number, the solution was oscillating. Then we increased the number of grids to 513×513 . This time we were able to obtain steady solutions up to $\text{Re} \leq 15,000$. With using this many number of grids, one thing is important to note, at Reynolds number of 17,500 when sufficiently small relaxation parameters that would not let the code to diverge were used, the solution was not converging but it was oscillating again. Erturk et. al. [12] have obtained the same type of behavior and they have stated that when they increased the number of grids used, they were able to obtain a converged solution. In this study, we then decided to increase the number of grids to 1025×1025 . This time we were able to obtain converged steady solutions up to Reynolds

number of 20,000. We note that with this many number of grids we could not obtain a solution for 21,000 as Erturk et. al. [12] have obtained. The solution at $Re=21,000$ was oscillating again when sufficiently small relaxation parameters were used. This suggests that, most probably, when a larger grid mesh is used the steady computations are possible, however, we did not attempt to increase the number of grids further beyond 1025×1025 .

For a given Reynolds number, we have used the same β values for both streamfunction and vorticity equations (3 and 5) and these β values are tabulated in Table 1. We note that we did not try to obtain the optimum β values at a given Reynolds number that would offer the fastest convergence since it was not the purpose. What we did was, when the solution diverged we decreased the value of β by 0.1.

Figure 2 and Figure 3 show the streamfunction and vorticity contours of the cavity flow up to $Re \leq 20,000$ with 1025×1025 grid mesh. These contour figures show that, the fine grid mesh provides very smooth solutions at high Reynolds numbers.

The location of the primary and the secondary vortices and also the streamfunction (ψ) and vorticity (ω) values at these locations are tabulated in Table 2. These results are in good agreement with Erturk et. al. [12]. They have stated that they have observed the quaternary vortex at the bottom left corner, BL3, appear in the solution at $Re=10,000$ when fine grids (600×600) were used. In this study we found that, when a more fine grid mesh (1025×1025) is used, BL3 vortex appear in the solution at $Re=7,500$. This would then suggest that in order to resolve the flow at high Reynolds numbers, fine grids are necessary.

Figure 4 and 5 show the u-velocity distribution along a vertical line and the v-velocity along a horizontal line passing through the center of the cavity respectively, at various Reynolds numbers. Detailed quantitative results obtained using a fine grid mesh was tabulated extensively in Erturk et. al. [12], therefore quantitative tabulated results will not be repeated in this study. The results obtained in this study agrees well with Erturk et. al. [12] and the reader is referred to that study for quantitative results. The reason why we choose to plot the u- and v-velocity profiles in Figures 4 and 5 is that, since the considered flow in cavity is incompressible we can use these velocity profiles to test the accuracy of the solution. If there exists a solution to the 2-D steady incompressible equations at high Reynolds numbers, then this solution must satisfy the continuity of the fluid. The continuity will provide a very good mathematical check on the solution as it was suggested first by Aydin & Fenner [3]. As seen in Figures 4 and 5 the integration of these velocity profiles will give the plus and minus areas shown by grey colors. The degree to which the plus and minus areas cancel each other such that the integration gives a value close to zero, will be an indicative of the mathematical accuracy of the solution. The velocity profiles are integrated using Simpson's rule to obtain the net volumetric flow rate Q passing through these sections. The obtained volumetric flow rates are then normalized by a characteristic flow rate which is the horizontal rate (Q_c) that would occur in the absence of the side walls (Plane Couette flow), to help quantify the errors. The obtained volumetric flow rate values ($Q_1 = \frac{|\int_0^1 u dy|}{Q_c}$ and $Q_2 = \frac{|\int_0^1 v dx|}{Q_c}$) are tabulated in Table 3. The volumetric flow rates in Table 3 are so small that they can be considered as $Q_1 \approx Q_2 \approx 0$. This mathematical check on the conservation of the continuity shows that our numerical solution is indeed very accurate.

4. DISCUSSIONS

The driven cavity flow problem has three aspects; physical (hydrodynamic), mathematical and numerical (computational) aspects and we think that the problem has to be analyzed in terms of these aspects *separately*.

We note that a very brief discussion on computational and also experimental studies on driven cavity flow can be found on Shankar & Deshpande [38]. First let us analyze the physical aspects of the cavity flow and look at the experimental studies.

Koseff & Street [25, 26, 27], Prasad & Koseff [33] have done several experiments on three dimensional driven cavity with various spanwise aspect ratios (SAR). Their experiments ([25, 26, 27, 33]) have shown that the flow in a cavity exhibit both local and global three-dimensional features. For example in a local sense they have found that Taylor-Goertler-Like (TGL) vortices form in the region of the Downstream Secondary Eddy (DSE). Also corner vortices form at the cavity end walls. In a global scale, due to no slip boundary condition on the end walls the flow is three-dimensional. They ([25, 26, 27, 33]) concluded that two-dimensional cavity flow does not exist (up to SAR=3) and further more, the presence of the TGL vortices precludes the possibility that the flow will be two dimensional even at large SAR. These conclusions clearly show that a two dimensional approximation for the flow in a cavity breaks down physically even at moderate Reynolds numbers.

Their results ([25, 26, 27, 33]) have also shown that the flow is laminar but unsteady even at moderate Reynolds numbers. The flow starts to show the signs of turbulence characteristics with turbulent bursts between $6,000 \leq Re \leq 8,000$. Above Reynolds number of 8,000 the flow in a cavity is turbulent (for SAR=3).

According to these valuable physical information provided by [25, 26, 27, 33], the fact of the matter is, the flow in cavity is neither two-dimensional nor steady at high Reynolds numbers. Since two-dimensional steady flow in a cavity at high Reynolds numbers does not occur in reality, this flow (ie. 2-D steady cavity flow at high Re) is a fictitious flow, as it is also concluded by Shankar & Deshpande [38]. This is a very important fact to remember.

In our computations, as a starting point we have assumed that the flow inside a cavity is two-dimensional, therefore, we have used the 2-D Navier-Stokes equations and all of the solutions presented are based on the assumption that the flow is two-dimensional. This is also the case in most computational studies on driven cavity flow. At this point we should question whether or not an incompressible flow inside a cavity be two-dimensional at high Reynolds numbers. Let us consider a 3-D cavity with a moderate spanwise aspect ratio (SAR). In this cavity, as the Reynolds number increases up to some Reynolds numbers, the flow at the symmetry plane (at the center in z-axis) could be assumed two dimensional. However after some Reynolds number the walls in third dimension (z-direction) will start to affect the flow due to non-slip condition (end-wall-effects). Above these Reynolds numbers, physically, the flow inside this cavity can not be assumed two dimensional. If we use a different cavity with a larger aspect ratio, still, after some Reynolds number the third dimensional effects cannot be ignored and a 2-D assumption fails after these Reynolds numbers. Now let us assume that hypothetically we have a cavity with an infinite aspect ratio ($SAR \rightarrow \infty$), then in terms of the end-wall-effects, only in this case the flow can be assumed purely two dimensional at high Reynolds numbers, and this is a fictitious scenario. We note that, here we look at the cavity flow only on a global scale and consider only the end-wall-effects. Kim & Moin [24] have numerically simulated the three-dimensional time dependent flow in a square cavity with using periodic boundary

conditions in the spanwise direction. They have observed TGL vortices in the flow field even though they did not have end walls in their simulations. Their results are important in the fact that in driven cavity flow the TGL vortices do not even need end walls to initiate. Experimental studies, [25, 26, 27, 33], also show that, in local scale TGL vortices appear in the region of the downstream secondary eddy (DSE). Therefore, even the flow in an infinite aspect ratio cavity will not be two-dimensional physically due to the TGL vortices.

As a conclusion, physically, at high Reynolds numbers two dimensional cavity flow does not exist and any study that considers a two dimensional flow at high Reynolds numbers, is dealing with a fictitious flow.

Now let us analyze the cavity flow mathematically and also numerically. In our computations, we have used 2-D Navier Stokes equations, and also we have presented *steady* solutions of the cavity flow at high Reynolds numbers. In light of these two points, what could be the nature of the flow at high Reynolds numbers? Mathematically speaking a two-dimensional flow cannot be turbulent. Turbulence is by nature three-dimensional and is not steady. Therefore due to our two-dimensional assumption, mathematically the flow could not be turbulent. Since, when 2-D equations are used and therefore we do not let the flow be turbulent mathematically, could the flow still be time dependent, ie. periodic? Although 2-D high Reynolds number scenario is fictitious, this is a legitimate question in terms of a mathematical and numerical analysis. At this point we are trying to answer the mathematical and numerical nature of a fictitious flow and see if there exists a steady solution to 2-D Navier-Stokes equations or not. Mathematically speaking, a two-dimensional flow can be either steady (ie. solution is independent of time) or unsteady but time dependent (ie. solution is periodic in time) or unsteady but time independent (ie. solution is completely chaotic). Since there is a possibility that the flow could be either steady or unsteady, then is the flow in cavity steady or unsteady, or in other words does a steady solution exists to 2-D Navier-Stokes equations or not? In the literature it is possible to find studies that present steady solutions of 2-D incompressible Navier-Stokes equations at high Reynolds numbers and the studies of Erturk et. al. [12], Erturk and Gokcol [13], Barragy & Carey [4], Schreiber & Keller [37], Benjamin & Denny [6], Liao & Zhu [28], Ghia et. al. [21] can be counted as example. In the literature there are also studies that claim the two dimensional cavity flow is unsteady, the studies in second and third category mentioned in the introduction can be counted as example.

As mentioned earlier, in the second category studies, researchers have tried to obtain the Reynolds number at which a Hopf bifurcation occurs in the flow, ie. the Reynolds number at which the flow changes from steady to unsteady characteristics. In these studies, the basic steady cavity flow solution is perturbed with small disturbances and then the eigenvalues of linearized Navier-Stokes equations are analyzed via hydrodynamic stability analysis.

Both external and internal flows, as Reynolds number is increased, exhibit a change from laminar to turbulent regime. In order to determine the Reynolds number that the transition from laminar to turbulent flow occurs, the Stability Theory is used. According to Stability Theory, in investigating the stability of laminar flows, the flow is decomposed into a basic flow whose stability is to be examined and a superimposed perturbation flow. The basic flow quantities are steady and the perturbation quantities vary in time. These basic and perturbation variables are inserted into Navier-Stokes equations. Assuming that

the perturbations are small, equations are linearized and using a normal mode form for these perturbations, an Orr-Sommerfeld type of equation is obtained. The stability of a laminar flow becomes an eigenvalue problem of the ordinary differential perturbation equation. If the sign of imaginary part of the complex eigenvalue smaller than zero then the flow is stable, if it is greater than zero the flow is unstable (see Schlichting & Gersten [36] and also Drazin & Reid [11]).

In the case of driven cavity flow, the stability analysis requires solving the partial differential eigenvalue problem. Fortin et. al. [19], Gervais et. al. [20], Sahin & Owens [35] and Abouhamza & Pierre [1] are examples of hydrodynamic stability studies on driven cavity flow found in the literature. In these studies ([19, 20, 35, 1]), a two-dimensional basic flow is considered and then the solution of this two-dimensional basic flow is obtained numerically. Then this solution is perturbed with two-dimensional disturbances. The perturbation problem at hand is a partial differential eigenvalue problem, therefore the eigenvalues are also obtained numerically. These studies predict that a Hopf bifurcation takes place in a 2-D incompressible flow in a driven cavity some where around Reynolds number of 8,000.

One important point is that, the accuracy of the solution of the perturbation equation (or eigenvalues) completely depend on the accuracy of the solution of the basic flow. Since the perturbation quantities are assumed to be small compared to the basic flow quantities, any negligible numerical errors will greatly affect the solution of the perturbation equation (Haddad & Corke [23], Erturk & Corke [14], Erturk et. al. [15]). Therefore for the sake of the accuracy of the solution of the perturbation equations, a highly accurate basic flow solution is required. In hydrodynamic analysis studies of driven cavity flow ([19, 20, 35, 1]) the number of grid points used is less than 257×257 . Erturk et. al. [12] have reported that when a grid mesh with less than 257×257 points is used in cavity flow, the solution start to oscillate around Reynolds number range $7500 \leq Re \leq 12500$ depending on the order of the boundary conditions used at the wall. We note that the Reynolds numbers predicted by [19, 20, 35, 1] for Hopf bifurcation is in the range, reported by Erturk et. al. [12], where the solution becomes oscillatory due to coarse grid mesh (ie. large Peclet number). We believe that in these studies ([19, 20, 35, 1]), when the considered Reynolds number is close to the Reynolds number where the basic solution becomes oscillatory due to numerical instability, the solution of the perturbation equation is affected by this numerical instability in the basic flow.

Most importantly, a hydrodynamic analysis would only be useful and also meaningful when there exists a physical flow otherwise the results of such a study would be physically useless. The experiments of Koseff & Street [25, 26, 27] and Prasad & Koseff [33] have shown that the flow inside a cavity is neither two-dimensional nor steady even at moderate Reynolds numbers. Therefore the results of a strictly two-dimensional hydrodynamic analysis (two-dimensional basic flow with two-dimensional perturbations) of a fictitious cavity flow will be also fictitious and will have no physical meaning.

Apart from the studies that examine the hydrodynamic stability of the driven cavity flow by considering a two-dimensional basic flow perturbed with two-dimensional disturbances mentioned above, the studies of Ramanan & Homsy [34] and Ding & Kawahara [10] are quite interesting and important. Both studies have considered a two-dimensional flow for driven cavity and analyzed when this two-dimensional basic flow is perturbed with three-dimensional disturbances. Ramanan & Homsy [34] found that the two di-

dimensional flow loses stability at $Re=594$ when perturbed with three-dimensional disturbances, whereas Ding & Kawahara [10] have predicted the instability at $Re=1025$ with a frequency of 0.8. We believe that the results of Ding & Kawahara [10] greatly over estimates the critical Reynolds number since they have used a slight compressibility in their simulations, such that their results are not purely incompressible. Note that these critical Reynolds numbers obtained with considering two-dimensional basic flow perturbed with three-dimensional disturbances ([10, 34]) are much lower than the critical Reynolds numbers obtained with the strictly two-dimensional hydrodynamic analysis ([19, 20, 35, 1]) in which a two-dimensional basic flow perturbed with two-dimensional disturbances is considered. This is very important such that, the results of Ramanan & Homsy [34] and Ding & Kawahara [10] show that, for the hydrodynamic stability of driven cavity flow the spanwise modes are more dangerous than the two dimensional modes. Also note that, their results ([34, 10]) do not include the effect of the end walls in spanwise direction. We expect that with including the effect of end walls and the TGL vortices, a three-dimensional flow analysis will have a lower critical Reynolds number for stability when perturbed with three-dimensional disturbances.

As mentioned earlier, in the third category studies, researchers have tried to obtain the Reynolds number that the flow experience a transition from a steady regime to an unsteady regime. In these studies, first a Reynolds number is considered, if a steady solution is obtained then the flow is solved for a higher Reynolds number until a periodic solution is obtained. By doing several runs, the exact transition Reynolds number at which the solution changes characteristics from steady to unsteady behavior, is obtained. The following studies are example of DNS studies found in the literature.

Auteri, Parolini & Quartepelle [2] have used a second order spectral projection method. With this they have solved the Unsteady 2-D N-S equations in primitive variables. They have analyzed the stability of the driven cavity with an impulsively started lid using 160×160 grids. They have removed the singularity that occurs at the corners of the cavity. They have increased the Reynolds number step by step until the solution becomes periodic. They have found that a Hopf bifurcation occurs in the interval $Re=8,017.6-8,018.8$. At this Reynolds number their solution was periodic with a frequency of 0.4496. They also reported that the cavity flow passes through a second Hopf bifurcation in the interval $Re=9,687-9,765$.

Peng, Shiau & Hwang [30] have used a Direct Numerical Simulation (DNS) by solving the 2-D unsteady Navier-Stokes equations in primitive variables. With using a maximum of 200×200 grids, they have solved the cavity flow by increasing the Reynolds number. At $Re=7,402 \pm 4$ their solutions became periodic with a certain frequency of 0.59. As Re was increased to 10,300 the flow became a quasi-periodic regime. When the Re was increased to 10,325 the flow returned to a periodic regime again. Between Reynolds numbers of 10,325 and 10,700 the flow experienced an inverse period doubling and between 10,600 and 10,900 the flow experienced a period doubling. Finally they claimed that the flow becomes chaotic when Re was greater than 11,000.

Tiesinga, Wubs & Veldman [42] have used Newton-Picard method and recursive projection method using a 128×128 grid mesh and with these they claimed that in a 2-D incompressible flow inside a cavity the first a Hopf bifurcation occurs at $Re=8,375$ with a frequency of 0.44. The next Hopf bifurcations occur at $Re=8,600, 9,000, 9,100$ and $10,000$ with frequencies 0.44, 0.53, 0.60 and 0.70. At these intervals the flow is either stable

periodic or unstable periodic.

Poliašenko & Aidun [32] have used a direct method based on time integration. Using Newton iterations with 57×57 number of grid points they have claimed that a Hopf bifurcation occurs in a lid driven cavity at $Re=7,763 \pm 2\%$ with a frequency of $2.86 \pm 1\%$. They have stated that this Hopf bifurcation is supercritical.

Cazemier, Verstappen & Veldman [8] have used Proper Orthogonal Decomposition (POD) and analyzed the stability of the cavity flow. They compute the first 80 POD modes, which on average capture 95% of the fluctuating kinetic energy, from 700 snapshots that are taken from a Direct Numerical Simulation (DNS). They have stated that the first Hopf bifurcation take place at $Re=7,819$ with a frequency of about 3.85.

Goyon [22] have solved 2-D unsteady Navier-Stokes equations in streamfunction and vorticity variables using Incremental Unknowns with a maximum mesh size of 257×257 . They have stated that a Hopf bifurcation appears at a critical Reynolds number between 7,500 to 10,000. They have presented periodic asymptotic solutions for $Re=10,000$ and 12,500.

Wan, Zhou & Wei [44] have solved the 2-D incompressible Navier-Stokes equations with using a Discrete Singular Convolution method on a 201×201 grid mesh. Also Liffman [29] have used a Collocation Spectral Solver and solved the 2-D incompressible Navier-Stokes with 64×64 collocation points. Both studies claimed that the flow in a cavity is periodic at Reynolds number of 10,000.

These are just example studies we picked from the literature that uses Direct Numerical Simulation (DNS) to capture the critical Reynolds number that a Hopf bifurcation occurs in a driven cavity flow.

Let us imagine that the 2-D incompressible flow inside a cavity is not stable at a given Reynolds number, such that a steady solution does not exist and the solution is time dependent. In this case, if one have used the steady N-S equations then one should not obtain a solution since there is no steady state solution.

Now let us imagine the opposite, such that, the 2-D incompressible flow inside a cavity is stable at a given Reynolds number. In this case the flow is steady and a steady solution does exist. If one have used the steady N-S equations and obtain a numerical solution, then the solution of unsteady N-S equations should converge to this solution through iterations in time also. We note that the boundary conditions are independent of time. Therefore, if there exist a unique solution to steady equations then solution of unsteady equations should converge to this solution also, since there is nothing to drive the solution vary in time because the boundary conditions are steady and also a steady solution of governing equations exists. In this case if the solution of unsteady equations do not converge to a steady solution then this would indicate that there are numerical stability issues with the solution of the unsteady equations and the time dependent periodic solution or any other solution obtained that is different than the steady solution should not be trusted.

Erturk et. al. [12] have reported that at high Reynolds numbers when they have used a grid mesh of 257×257 , they observed that their solutions oscillate in the pseudo time. However, when they have used a larger grid mesh than 257×257 , they were able to obtain a steady solution at high Reynolds numbers. In this study, when we have used a grid mesh of 257×257 , at high Reynolds numbers the solution was not converging to a steady state but it was oscillating, even when very small relaxation parameters (β) were used. However when we have increased the grid mesh to 513×513 , we were able to obtain steady solutions

up to $Re=15,000$. With this many number of grid points, above this Reynolds number, the solution started to oscillate again even when sufficiently small relaxation parameters that would not allow the solution to diverge were used. And when we have increased the grid points up to 1025×1025 , again we were able to obtain steady solutions up to $Re=20,000$. Therefore based on the experiences of Erturk et. al. [12] and this study, we conclude that in order to obtain a steady solution for the driven cavity flow a grid mesh larger than 257×257 is necessary when high Reynolds numbers are considered and also at high Reynolds numbers when a coarse grid mesh is used then the solution oscillates. The interesting thing is that, both in this study and in Erturk et. al. [12], the obtained false periodic numerical solutions looked so real and fascinating with certain frequencies and periodicity. We believe that the studies that presented unsteady solutions using Direct Numerical Simulations, [2, 30, 42, 32, 8, 22, 44, 29], have experienced the same type of numerical oscillations because they have used a small grid mesh. Our very detailed literature survey showed that, in all the numerical studies of driven cavity flow, above Reynolds number of 5,000, the maximum number of grid points used is 257×257 . Larger grid meshes have never been used in studies above $Re=5,000$. We think that, a Direct Numerical Simulation (DNS) algorithm would also confirm the same results obtained in this study and in Erturk et. al. [12] when sufficiently large grid meshes are used. As Erturk et. al. [12] have stated, one of the reasons, why the steady solutions of the driven cavity flow at very high Reynolds numbers become computable when finer grids are used, may be the fact that as the number of grids used increases, Δh gets smaller, then the cell Reynolds number or so called Peclet number defined as $Re_c = \frac{u\Delta h}{\nu}$ decreases. This improves the numerical stability characteristics of the numerical scheme used ([41, 45]), and allows high cavity Reynolds number solutions computable. Another reason may be that fact that finer grids would resolve the corner vortices better. This would, then, help decrease any numerical oscillations that might occur at the corners of the cavity during iterations. When we have used a coarse grid mesh in our solutions, the oscillations we observed looked so real that they could easily be mistaken deceptively as the real time behavior of the flow field. One may think that if the numerical simulation of time dependent equations (DNS) do not converge to steady state, then the flow is not hydrodynamically stable. However one should not forget that a DNS is also restricted with certain numerical stability conditions, such as a Peclet number restriction in driven cavity flow as explained. We believe that DNS should not be used to predict the transition Reynolds number or Hopf bifurcation Reynolds numbers in a flow field because any numerical oscillations in the solution due to numerical stability issues can easily be confused as the hydrodynamic oscillations.

The two dimensional cavity flow at high Reynolds number is a fictitious flow. Mathematically and numerically it is possible to study fictitious flows and in the literature it is possible to find many fictitious flows that are subject of mathematical and numerical studies. For example the 2-D incompressible flow over a circular cylinder is steady for Reynolds number up to approximately 40. Beyond that Reynolds number there appears Karman vortex street at downstream of the cylinder and the physical ie. the real flow is unsteady. A steady solution beyond $Re=40$, if exists, is fictitious. However for this flow case, the 2-D incompressible flow over a cylinder, it is possible to obtain a steady solution mathematically when Re goes to infinity as the limiting solution (Kirchoff-Helmholtz solution, see Schlichting & Gersten [36]). Smith [39] and Peregrine [31] have done detailed mathematical analysis on this fictitious flow at Reynolds numbers higher than 40. Forn-

berg [17, 18], Son & Hanratty [40], Tuann & Olson [43] and Dennis & Chang [9] have presented numerical solutions of steady flow past a circular cylinder at $Re=300, 600, 500, 100$ and 100 respectively, which are much larger than Reynolds number of 40 . This fact is important such that, even though the flow is physically fictitious, a mathematical solution exists and also it is possible to obtain a numerical solution as well. In this study the presented solutions clearly show that steady solutions exist for two dimensional driven cavity flow at high Reynolds numbers and these solutions are computable even with the simplest explicit algorithm, SOR, when finer grids are used.

5. CONCLUSIONS

In this study, the steady 2-D Navier-Stokes equations in streamfunction and vorticity formulation are solved numerically simply with using Successive-Over-Relaxation (SOR) algorithm. Our study shows that there exists a steady solution to the lid driven cavity flow at high Reynolds numbers and this solution is computable even with the simplest numerical method, SOR, provided that a fine grid mesh is used as suggested by Erturk et. al. [12]. The solutions of the cavity flow with using a 1025×1025 mesh showed that the quaternary vortex at the bottom left corner, BL3, appear in the solution at $Re=7,500$. Both the numerical residuals and also the mathematical continuity check prove that the presented numerical solutions are indeed very accurate.

In the present study we have also discussed several studies on the driven cavity flow in terms of physical, mathematical and numerical aspects and we deduced the followings:

1. Experiments showed that, physically, the flow in a driven cavity is not two dimensional and is not steady most probably even at $Re=1000$.
2. At high Reynolds numbers when the incompressible flow in a square cavity is considered as two-dimensional and also steady, then the considered flow is a fictitious flow.
3. It would be meaningless to study the hydrodynamic stability of a fictitious flow such as the two-dimensional incompressible cavity flow, especially when perturbed with two-dimensional disturbances. On the other hand studies with two-dimensional cavity flow perturbed with three-dimensional disturbances predict significantly different results compared to the former two-dimensional perturbation approach, and their results compare good with the experiments.
4. Direct Numerical Simulation (DNS) should not be used in obtaining the hydrodynamic stability (ie. the critical Reynolds number) of a fluid flow problem. There is always a chance that the oscillations in the solution could be due to the numerical instability and these oscillations could be easily mistaken as the real physics of the flow.
5. Mathematically, it is always possible to obtain a steady solution of a fictitious flow at the limiting case when Re goes to infinity. As shown in Erturk et. al. [12], Bachelor's [5] model of recirculating flow confined in closed streamlines at infinite Reynolds number seems to work with the square driven cavity flow. The numerical

solutions of Erturk et. al. [12] agrees well with the analytical solutions of Burggraf [7].

6. Numerically, it is possible to obtain numerical solutions of 2-D steady incompressible cavity flow at high Reynolds numbers even with using the simplest algorithm, SOR, when fine grid meshes are used.
7. The model flow problem, the 2-D steady incompressible driven cavity flow serve as a good benchmark problem for different numerical methods and boundary conditions, in terms of accuracy, convergence rate and etc., provided that these numerical solutions should only be used for numerical comparison purposes between different solutions or with the analytical solution. The presented solutions in this study provide highly accurate, fine grid benchmark solutions for future references.

Acknowledgment

This study was funded by Gebze Institute of Technology with project no BAP-2003-A-22. E. Ertürk is grateful for this financial support.

References

- [1] A. Abouhamza and R. Pierre, A Neutral Stability Curve for Incompressible Flows in a Rectangular Driven Cavity, *Mathematical and Computer Modelling* **38** (2003) 141–157.
- [2] F. Auteri, N. Parolini and L. Quartapelle, Numerical Investigation on the Stability of Singular Driven Cavity Flow, *Journal of Computational Physics* **183** (2002) 1–25.
- [3] M. Aydin and R.T. Fenner, Boundary Element Analysis of Driven Cavity Flow for Low and Moderate Reynolds Numbers, *International Journal for Numerical Methods in Fluids* **37** (2001) 45–64.
- [4] E. Baragy and G.F. Carey, Stream Function-Vorticity Driven Cavity Solutions Using p Finite Elements, *Computers and Fluids* **26** (1997) 453–468.
- [5] G.K. Batchelor, On Steady Laminar Flow with Closed Streamlines at Large Reynolds Numbers, *Journal of Fluid Mechanics* **1** (1956) 177–190.
- [6] A.S. Benjamin and V.E. Denny, On the Convergence of Numerical Solutions for 2-D Flows in a Cavity at Large Re , *Journal of Computational Physics* **33** (1979) 340–358.
- [7] O.R. Burggraf, Analytical and Numerical Studies of the Structure of Steady Separated Flows, *Journal of Fluid Mechanics* **24** (1966) 113–151.
- [8] W. Cazemier, R.W.C.P. Verstappen and A.E.P. Veldman, Proper Orthogonal Decomposition and Low-Dimensional Models for the Driven Cavity Flows, *Physics of Fluids* **10** (1998) 1685–1699.

- [9] S.C.R. Dennis and G-Z. Chang, Numerical Solutions for Steady Flow Past a Circular Cylinder at Reynolds Numbers up to 100, *Journal of Fluid Mechanics* **42** (1970) 471–489.
- [10] Y. Ding and M. Kawahara, Linear Stability of Incompressible Fluid Flow in a Cavity Using Finite Element Method, *International Journal for Numerical Methods in Fluids* **27** (1998) 139–157.
- [11] P.G. Drazin and W.H. Reid, *Hydrodynamic Stability* Cambridge University Press, 1991.
- [12] E. Erturk, T.C. Corke and C. Gokcol, Numerical Solutions of 2-D Steady Incompressible Driven Cavity Flow at High Reynolds Numbers, *International Journal for Numerical Methods in Fluids* **48** (2005) 747–774.
- [13] E. Erturk and C. Gokcol, Fourth-Order Compact Formulation of NavierStokes Equations and Driven Cavity Flow at High Reynolds Numbers, *International Journal for Numerical Methods in Fluids* (2005) To Appear.
- [14] E. Erturk and T.C. Corke, Boundary layer leading-edge receptivity to sound at incidence angles, *Journal of Fluid Mechanics* **444** (2001) 383–407.
- [15] E. Erturk, O.M. Haddad and T.C. Corke, Numerical Solutions of Laminar Incompressible Flow Past Parabolic Bodies at Angles of Attack, *AIAA Journal* **42** (2004) 2254–2265.
- [16] C.A.J. Fletcher, *Computational Techniques for Fluid Dynamics* (2nd edn), Springer-Verlag, 1991.
- [17] B. Fornberg, A Numerical Study of Steady Viscous Flow Past a Circular Cylinder, *Journal of Fluid Mechanics* **98** (1980) 819–855.
- [18] B. Fornberg, Steady viscous flow past a circular cylinder up to Reynolds number 600, *Journal of Computational Physics* **61** (1985) 297–320.
- [19] A. Fortin, M. Jardak, J.J. Gervais and R. Pierre, Localization of Hopf Bifurcations in Fluid Flow Problems, *International Journal for Numerical Methods in Fluids* **24** (1997) 1185–1210.
- [20] J.J. Gervais, D. Lemelin and R. Pierre, Some Experiments with Stability Analysis of Discrete Incompressible Flows in the Lid-Driven Cavity, *International Journal for Numerical Methods in Fluids* **24** (1997) 477–492.
- [21] U. Ghia, K.N. Ghia and C.T. Shin, High-Re Solutions for Incompressible Flow Using the Navier-Stokes Equations and a Multigrid Method, *Journal of Computational Physics* **48** (1982) 387–411.
- [22] O. Goyon, High-Reynolds Number Solutions of Navier-Stokes Equations Using Incremental Unknowns, *Computer Methods in Applied Mechanics and Engineering* **130** (1996) 319–335.

- [23] O.M. Haddad and T.C. Corke, Boundary layer receptivity to free-stream sound on parabolic bodies, *Journal of Fluid Mechanics* **368** (1998) 1–26.
- [24] J. Kim and P. Moin, Application of a Fractional-Step Method to Incompressible Navier-Stokes Equations, *Journal of Computational Physics* **59** (1985) 308–323.
- [25] J.R. Koseff and R.L. Street, The Lid-Driven Cavity Flow: A Synthesis of Qualitative and Quantitative Observations, *ASME Journal of Fluids Engineering* **106** (1984) 390–398.
- [26] J.R. Koseff and R.L. Street, On End Wall Effects in a Lid Driven Cavity Flow, *ASME Journal of Fluids Engineering* **106** (1984) 385–389.
- [27] J.R. Koseff and R.L. Street, Visualization Studies of a Shear Driven Three-Dimensional Recirculating Flow, *ASME Journal of Fluids Engineering* **106** (1984) 21–29.
- [28] S.J. Liao and J.M. Zhu, A Short Note on Higher-Order Streamfunction-Vorticity Formulation of 2-D Steady State Navier-Stokes Equations, *International Journal for Numerical Methods in Fluids* **22** (1996) 1–9.
- [29] K. Liffman, Comments on a Collocation Spectral Solver for the Helmholtz Equation, *Journal of Computational Physics* **128** (1996) 254–258.
- [30] Y-H. Peng, Y-H. Shiau and R.R. Hwang, Transition in a 2-D Lid-Driven Cavity Flow, *Computers and Fluids* **32** (2003) 337–352.
- [31] D.H. Peregrine, A Note on the Steady High-Reynolds-Number Flow About a Circular Cylinder, *Journal of Fluid Mechanics* **157** (1985) 493–500.
- [32] M. Poliashenko and C.K. Aidun, A Direct Method for Computation of Simple Bifurcations, *Journal of Computational Physics* **121** (1995) 246–260.
- [33] A.K. Prasad and J.R. Koseff, Reynolds Number and End-Wall Effects on a Lid-Driven Cavity Flow, *Physics of Fluids A* **1** (1989) 208–218.
- [34] N. Ramanan and G.M. Homsy, Linear Stability of Lid-Driven Cavity Flow, *Physics of Fluids* **6** (1994) 2690–2701.
- [35] M. Sahin and R.G. Owens, A Novel Fully-Implicit Finite Volume Method Applied to the Lid-Driven Cavity Flow Problem. Part II. Linear Stability Analysis, *International Journal for Numerical Methods in Fluids* **42** (2003) 79–88.
- [36] H. Schlichting and K. Gersten, *Boundary Layer Theory* (8th revised and enlarged edn), Springer, 2000.
- [37] R. Schreiber and H.B. Keller, Driven Cavity Flows by Efficient Numerical Techniques, *Journal of Computational Physics* **49** (1983) 310–333.
- [38] P.N. Shankar and M.D. Deshpande, Fluid Mechanics in the Driven Cavity, *Annual Review of Fluid Mechanics* **32** (2000) 93–136.

- [39] F.T. Smith, A Structure for Laminar Flow Past a Bluff Body at High Reynolds Number, *Journal of Fluid Mechanics* **155** (1985) 175–191.
- [40] J.S. Son and T. Hanratty, Numerical Solution for the Flow Around a Cylinder at Reynolds Numbers of 40, 200 and 500, *Journal of Fluid Mechanics* **35** (1969) 369–386.
- [41] J.C. Tennehill, D.A. Anderson and R.H. Pletcher, *Computational Fluid Mechanics and Heat Transfer* (2nd edn), Taylor & Francis, 1997.
- [42] G. Tiesinga, F.W. Wubs and A.E.P. Veldman, Bifurcation Analysis of Incompressible Flow in a Driven Cavity by the Newton-Picard method, *Journal of Computational and Applied Mathematics* **140** (2002) 751–772.
- [43] S-Y. Tuann and M.D. Olson, Numerical Studies of the Flow Around a Circular Cylinder by a Finite Element Method, *Computers and Fluids* **6** (1978) 219–240.
- [44] D.C. Wan, Y.C. Zhou and G.W. Wei, Numerical Solution of Incompressible Flows by Discrete Singular Convolution, *International Journal for Numerical Methods in Fluids* **38** (2002) 789–810.
- [45] E. Weinan and L. Jian-Guo, Vorticity Boundary Condition and Related Issues for Finite Difference Schemes, *Journal of Computational Physics* **124** (1996) 368–382.

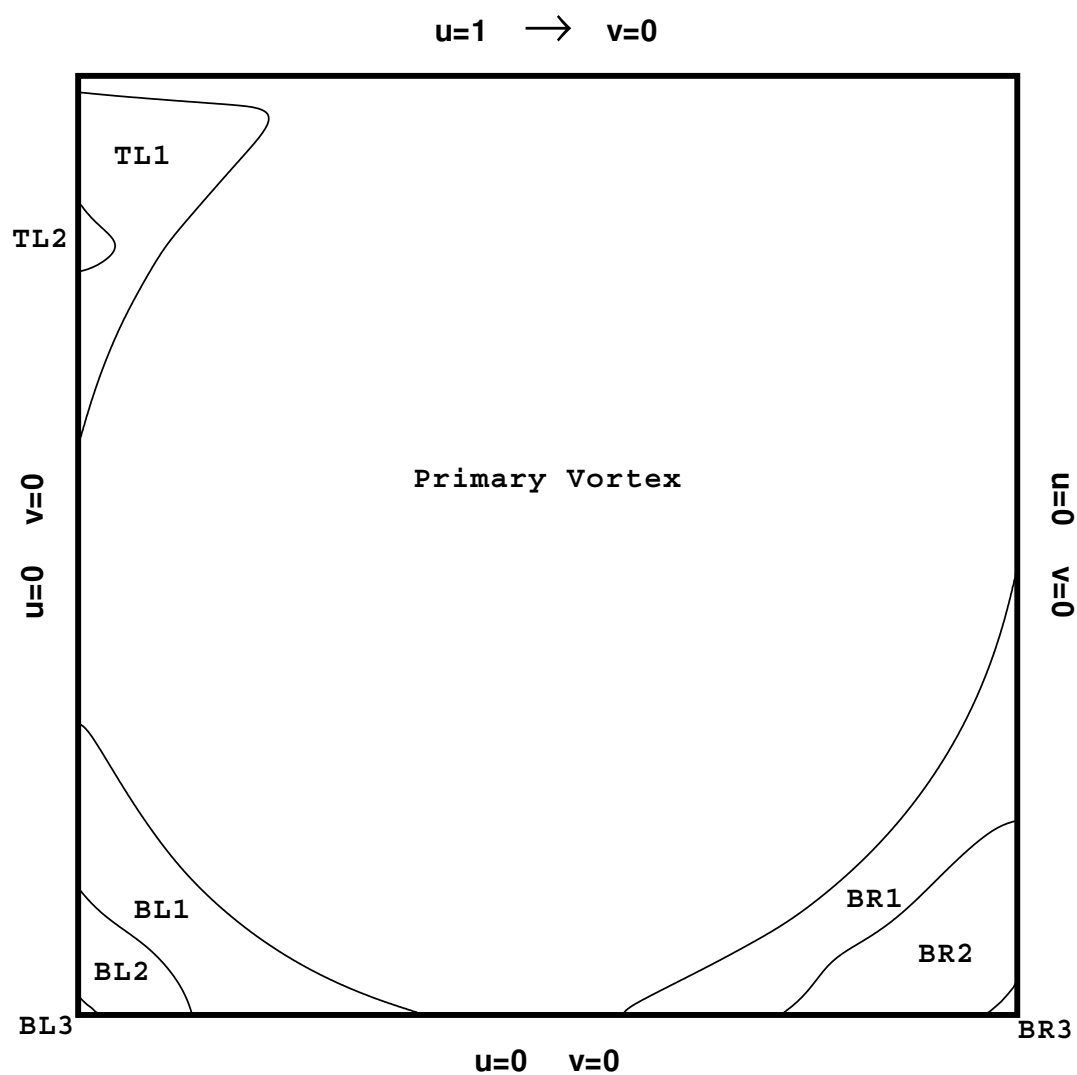


Figure 1. Schematic view of driven cavity flow

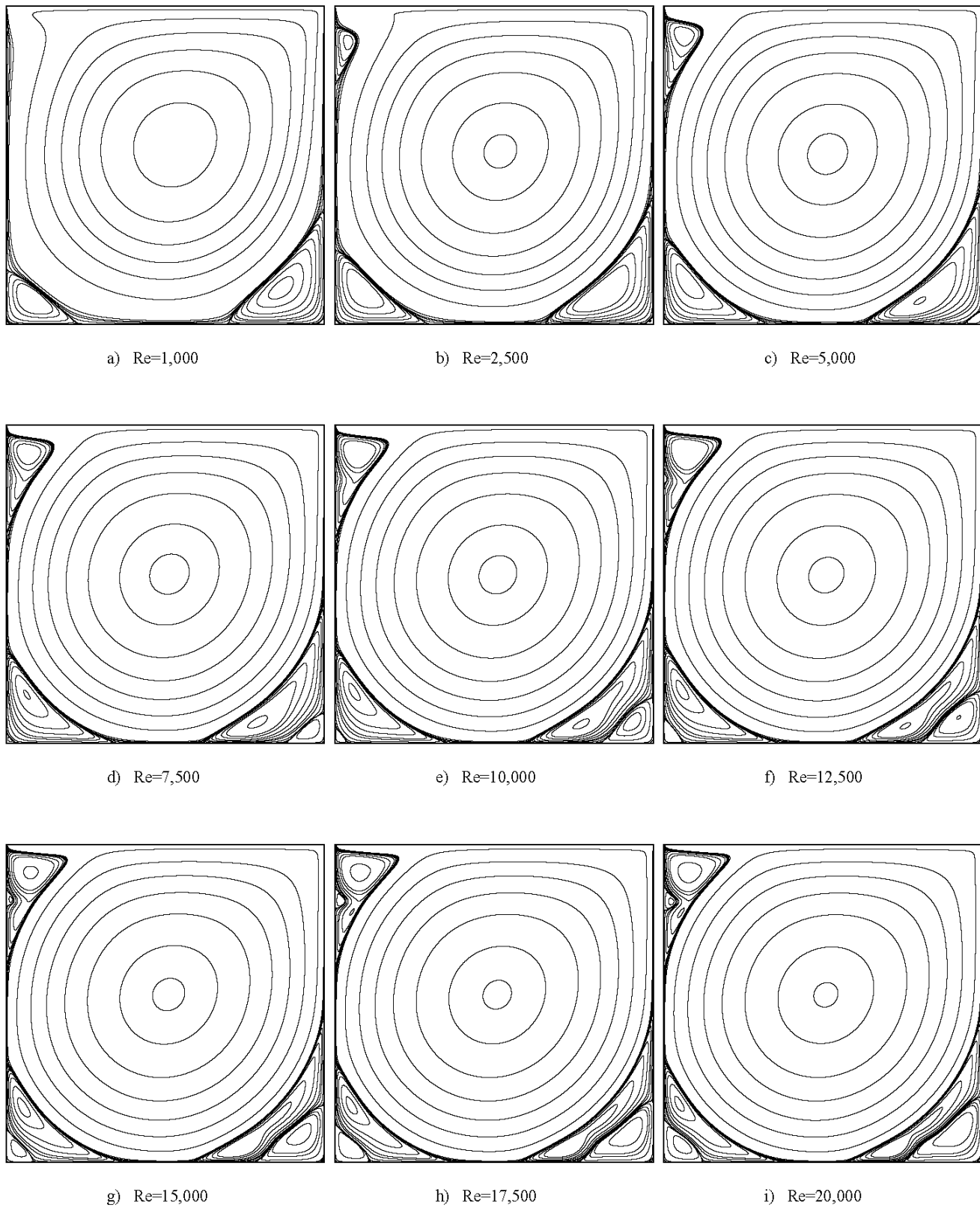
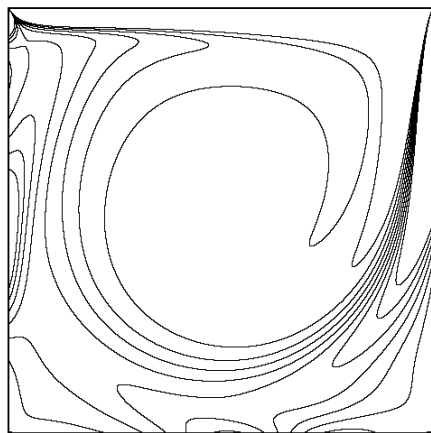
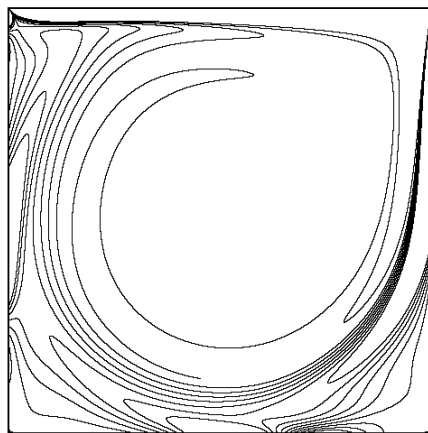


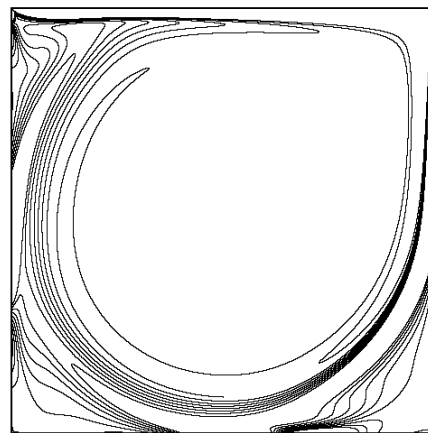
Figure 2. Streamfunction contours at various Reynolds numbers



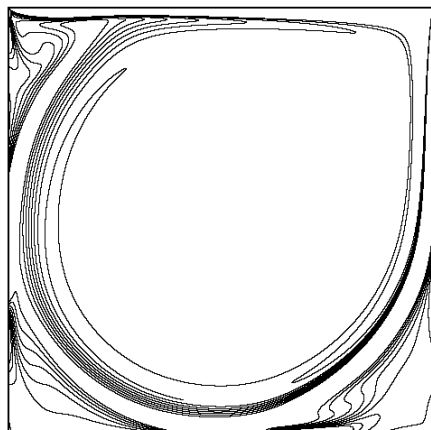
a) $Re=1,000$



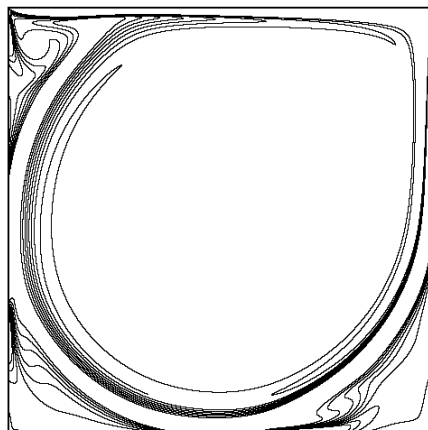
b) $Re=2,500$



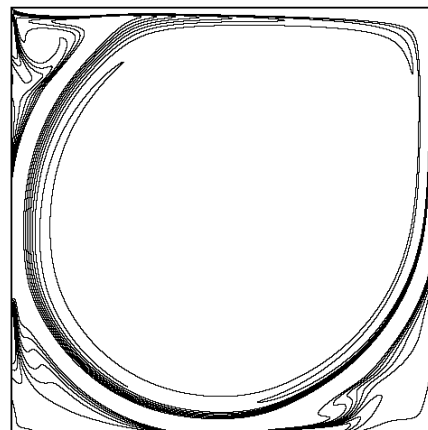
c) $Re=5,000$



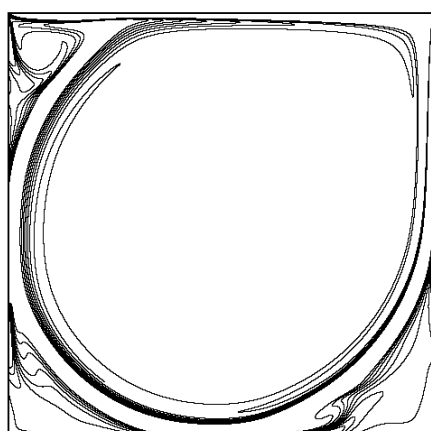
d) $Re=7,500$



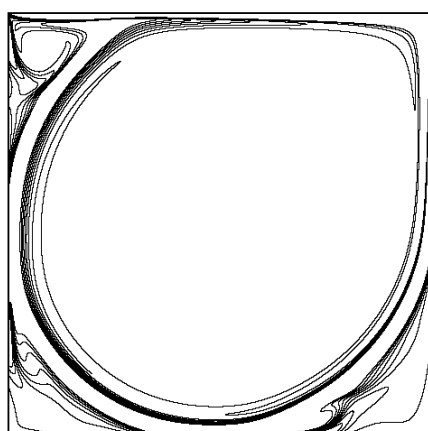
e) $Re=10,000$



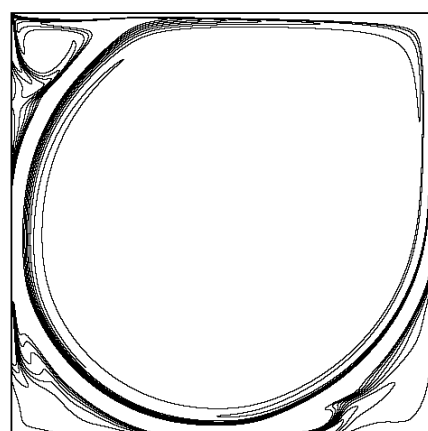
f) $Re=12,500$



g) $Re=15,000$



h) $Re=17,500$



i) $Re=20,000$

Figure 3. Vorticity contours at various Reynolds numbers

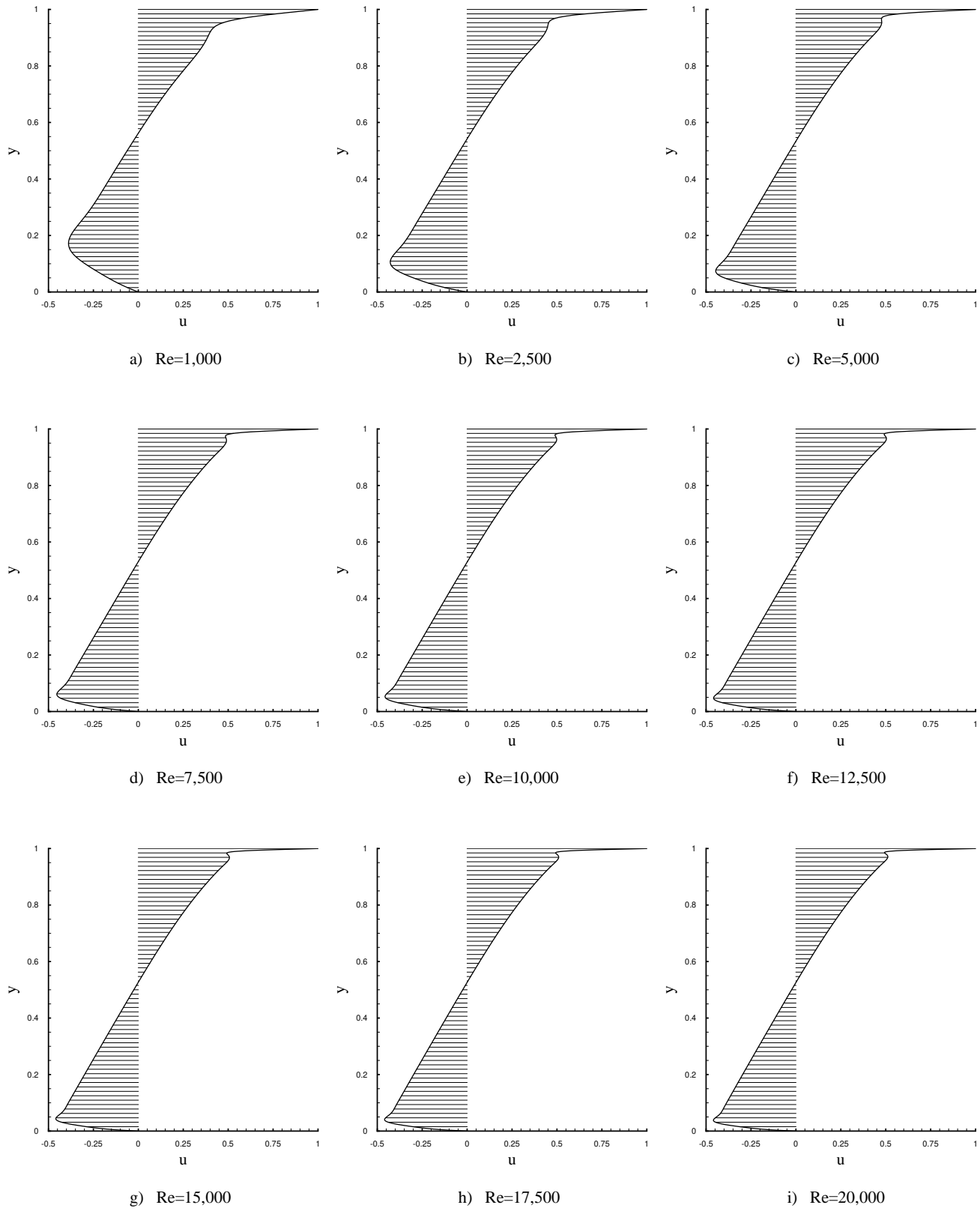


Figure 4. The u-velocity profiles along a vertical line passing through the center of the cavity

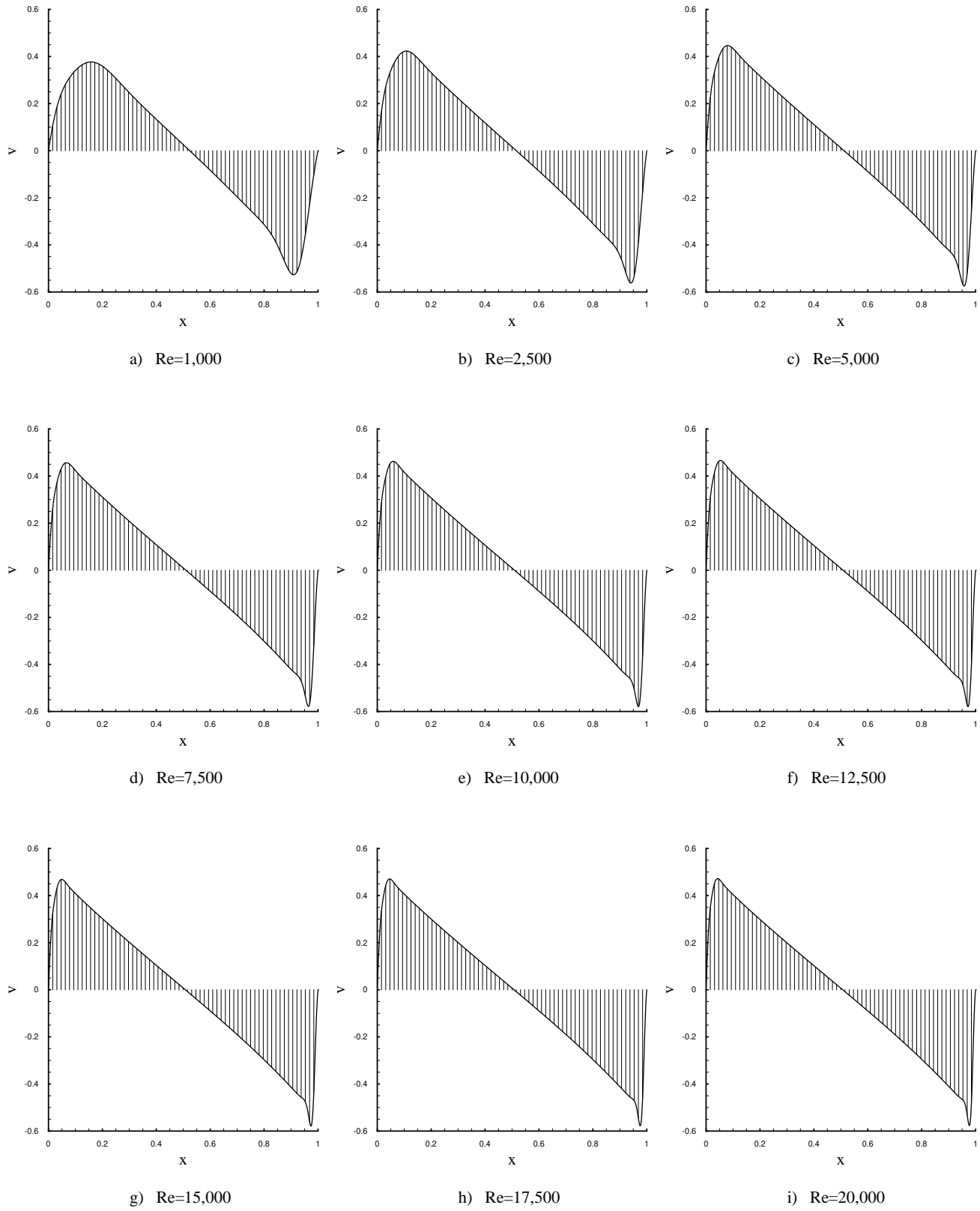


Figure 5. The v-velocity profiles along a horizontal line passing through the center of the cavity

Re	β
1000	1.2
2500	1.0
5000	0.8
7500	0.6
10000	0.5
12500	0.5
15000	0.4
17500	0.3
20000	0.3

Table 1. The relaxation parameter, β , used in SOR at various Reynolds numbers for 1025×1025 grid mesh

		Re	1000	2500	5000	7500	10000	12500	15000	17500	20000
Primary	ψ	-0.118888	-0.121337	-0.121942	-0.121939	-0.121781	-0.121571	-0.121342	-0.121105	-0.120865	-0.120865
Vortex	ω	-2.067052	-1.974087	-1.936291	-1.920053	-1.909677	-1.901830	-1.895353	-1.889712	-1.884630	-1.884630
	(x, y)	(0.5313 , 0.5654)	(0.5195 , 0.5439)	(0.5146 , 0.5352)	(0.5137 , 0.5322)	(0.5117 , 0.5303)	(0.5107 , 0.5283)	(0.5107 , 0.5283)	(0.5098 , 0.5273)	(0.5098 , 0.5264)	(0.5098 , 0.5264)
BR ₁	ψ	0.17287E-02	0.26594E-02	0.30677E-02	0.32198E-02	0.31846E-02	0.30930E-02	0.29991E-02	0.29019E-02	0.28038E-02	0.28038E-02
	ω	1.111550	1.923505	2.720926	3.216140	3.751749	4.355619	4.938041	5.504286	6.080160	6.080160
	(x, y)	(0.8643 , 0.1123)	(0.8350 , 0.0908)	(0.8057 , 0.0732)	(0.7910 , 0.0654)	(0.7754 , 0.0596)	(0.7607 , 0.0547)	(0.7471 , 0.0498)	(0.7354 , 0.0469)	(0.7246 , 0.0439)	(0.7246 , 0.0439)
BL ₁	ψ	0.23314E-03	0.92939E-03	0.13729E-02	0.15308E-02	0.16118E-02	0.16585E-02	0.16730E-02	0.16587E-02	0.16298E-02	0.16298E-02
	ω	0.350476	0.980549	1.510725	1.868003	2.145982	2.320998	2.507351	2.692707	2.932753	2.932753
	(x, y)	(0.0830 , 0.0781)	(0.0840 , 0.1113)	(0.0732 , 0.1367)	(0.0645 , 0.1523)	(0.0586 , 0.1621)	(0.0557 , 0.1670)	(0.0527 , 0.1719)	(0.0508 , 0.1768)	(0.0479 , 0.1826)	(0.0479 , 0.1826)
BR ₂	ψ	-0.50156E-07	-0.12139E-06	-0.14045E-05	-0.13991E-04	-0.13770E-03	-0.25203E-03	-0.33722E-03	-0.40202E-03	-0.45797E-03	-0.45797E-03
	ω	-0.89202E-02	-0.12542E-01	-0.34116E-01	-0.15359	-0.302428	-0.398521	-0.464422	-0.518223	-0.559633	-0.559633
	(x, y)	(0.9922 , 0.0078)	(0.9902 , 0.0088)	(0.9785 , 0.0186)	(0.9521 , 0.0420)	(0.9355 , 0.0674)	(0.9277 , 0.0811)	(0.9268 , 0.0889)	(0.9237 , 0.0967)	(0.9307 , 0.1045)	(0.9307 , 0.1045)
BL ₂	ψ	-0.63952E-08	-0.27624E-07	-0.66119E-07	-0.20023E-06	-0.10866E-05	-0.64356E-05	-0.22641E-04	-0.49066E-04	-0.82094E-04	-0.82094E-04
	ω	-0.27286E-02	-0.62456E-02	-0.99654E-02	-0.14650E-01	-0.31184E-01	-0.74967E-01	-0.140378	-0.200096	-0.250093	-0.250093
	(x, y)	(0.0049 , 0.0049)	(0.0059 , 0.0059)	(0.0078 , 0.0078)	(0.0107 , 0.0117)	(0.0166 , 0.0205)	(0.0264 , 0.0322)	(0.0381 , 0.0420)	(0.0498 , 0.0488)	(0.0586 , 0.0547)	(0.0586 , 0.0547)
TL ₁	ψ	-	0.34320E-03	0.14442E-02	0.21247E-02	0.26129E-02	0.29797E-02	0.32676E-02	0.35027E-02	0.37012E-02	0.37012E-02
	ω	-	1.315587	2.074175	2.231256	2.297052	2.350284	2.399048	2.437302	2.469835	2.469835
	(x, y)	(0.0430 , 0.8896)	(0.0635 , 0.9092)	(0.0664 , 0.9121)	(0.0703 , 0.9111)	(0.0742 , 0.9111)	(0.0771 , 0.9111)	(0.0791 , 0.9111)	(0.0801 , 0.9121)	(0.0801 , 0.9121)	(0.0801 , 0.9121)
BR ₃	ψ	-	-	0.42980E-10	0.84067E-09	0.38803E-08	0.76029E-08	0.11513E-07	0.17251E-07	0.26758E-07	0.26758E-07
	ω	-	-	0.11263E-03	0.14869E-02	0.21783E-02	0.35141E-02	0.41508E-02	0.45564E-02	0.55315E-02	0.55315E-02
	(x, y)	-	-	(0.9990 , 0.0010)	(0.9971 , 0.0029)	(0.9961 , 0.0039)	(0.9951 , 0.0049)	(0.9951 , 0.0059)	(0.9941 , 0.0059)	(0.9932 , 0.0068)	(0.9932 , 0.0068)
BL ₃	ψ	-	-	-	0.80824E-11	0.40286E-10	0.17663E-09	0.59435E-09	0.14160E-08	0.22536E-08	0.22536E-08
	ω	-	-	-	0.29106E-03	0.14243E-03	0.75527E-03	0.10105E-02	0.14427E-02	0.18191E-02	0.18191E-02
	(x, y)	-	-	-	(0.0010 , 0.0010)	(0.0010 , 0.0010)	(0.0020 , 0.0020)	(0.0020 , 0.0029)	(0.0029 , 0.0029)	(0.0039 , 0.0029)	(0.0039 , 0.0029)
TL ₂	ψ	-	-	-	-	-	-	-0.14694E-05	-0.15063E-04	-0.39746E-04	-0.68864E-04
	ω	-	-	-	-	-	-	-0.219588	-0.506032	-0.758492	-0.941342
	(x, y)	-	-	-	-	-	-	(0.0068 , 0.8311)	(0.0146 , 0.8262)	(0.0205 , 0.8223)	(0.0244 , 0.8203)

Table 2. Properties of primary and secondary vortices; streamfunction and vorticity values, (x, y) locations

Re	$Q_1 = \frac{ \int_0^1 u dy }{Q_c}$	$Q_2 = \frac{ \int_0^1 v dx }{Q_c}$
1000	2.451×10^{-10}	4.741×10^{-11}
2500	1.611×10^{-9}	2.550×10^{-10}
5000	5.625×10^{-9}	7.018×10^{-10}
7500	1.034×10^{-8}	9.813×10^{-10}
10000	1.411×10^{-8}	8.834×10^{-10}
12500	1.547×10^{-8}	2.795×10^{-10}
15000	1.313×10^{-8}	9.115×10^{-10}
17500	5.872×10^{-9}	2.743×10^{-9}
20000	7.364×10^{-9}	5.252×10^{-9}

Table 3. Volumetric flow rates through a vertical line, Q_1 , and a horizontal line, Q_2 , passing through the geometric center of the cavity